ELSEVIER

Journal of Molecular Catalysis A: Chemical 135 (1998) 99–106

JOURNAL OF MOLECULAR CATALYSIS A: CHEMICAL

Acidic property and catalytic behavior of chromium oxide–zirconia catalyst

Jong Rack Sohn [a,*], Sam Gon Ryu [a], Hae Won Kim [b]

[a] *Department of Industrial Chemistry, Engineering College, Kyungpook National University, Taegu 702-701, South Korea*
[b] *Department of Industrial Chemistry, Kyungil University, Kyungsan, 712-701, South Korea*

Received 23 January 1997; accepted 2 December 1997

Abstract

Chromium oxide–zirconia catalysts were prepared by dry impregnation of powdered $Zr(OH)_4$ with an aqueous solution of $(NH_4)_2CrO_4$ followed by calcining in air. Upon the addition of only a small amount of chromium oxide (1 wt.% Cr) to ZrO_2, both the acidity and acid strength of the catalyst increased remarkably, showing the presence of Brönsted and Lewis acid sites on the surface of CrO_x/ZrO_2. The catalytic behavior of the sample was investigated through the reaction of *n*-hexane using a pulse technique. It was found that Cr^{6+} species existing on the surface of catalyst was responsible for the formation of strong acid site and the cracking catalytic activity of *n*-hexane. However, the Cr^{6+} species was easily reduced to Cr^{3+} species during the catalytic reaction of *n*-hexane and the reduced Cr^{3+} species was active for benzene formation due to the dehydrocyclization of *n*-hexane. The reduced Cr^{3+} species could be reoxidized by treatment with O_2 and subsequently the reoxidized catalyst exhibited catalytic activity for the cracking reaction of *n*-hexane.

Keywords: Acidic property; Catalytic behavior; Chromium oxide–zirconia catalyst

1. Introduction

Supported chromium oxide catalysts are being used for the polymerization, hydrogenation, oxidation–reduction reactions between environmentally important molecules such as CO and NO [1–5]. Recently, many efforts have involved the characterization of these catalysts in an attempt to find the appropriate reaction mechanisms. The titrations to determine the oxidation state of the chromium used in conjunction with infrared and electron paramagnetic resonance spectroscopy have provided much information dealing with these question. So far, however, they have been studied mainly on silica and alumina [6–8], and only a small amount of work was done for the ZrO_2 support [9–11].

Zirconia is an important material due to its interesting thermal and mechanical properties, and so has been investigated as a support and catalysts in recent years. Different papers have been devoted to the study of ZrO_2 catalytic activity in important reactions such as methanol and hydrocarbon synthesis from CO and H_2 or CO_2 and H_2 [12,13] or alcohol dehydration [14,15]. Zirconia has been extensively used as a support for metals or incorporated in supports to

* Corresponding author.

1381-1169/98/$ - see front matter
PII: S1381-1169(97)00295-1

stabilize them or make them more resistant to sintering [16–18]. ZrO_2 activity and selectivity highly depend on the methods of preparation and the treatment used. In particular, in previous papers from this laboratory, it has been shown that $NiO–ZrO_2$ and ZrO_2 modified with sulfate ion are very active for acid-catalyzed reaction, even at room temperature [19–21]. The high catalytic activities in the above reaction were attributed to the enhanced acidic properties of the modified catalysts, which originate from the inductive effect of S=O bonds of the complex formed by the interaction of oxides with the sulfate ion.

It is well known that the dispersion, the oxidation state, and the structural features of supported species may strongly depend on the support. Structure and physicochemical properties of supported metal oxides are considered to be in different states compared with bulk metal oxides because of their interaction with supports. Previous paper described the surface characterization of chromium oxide supported on zirconia [22]. As an extension of study on supported catalyst, in this work, we deal with acidic property and catalytic behavior of chromium oxide–zirconia catalyst. For this purpose, *n*-hexane was used as a test reactant.

2. Experimental

2.1. Catalysts

The precipitate of $Zr(OH)_4$ was obtained by adding aqueous ammonia slowly into an aqueous solution of zirconium oxychloride at room temperature with stirring until the pH of the mother liquor reached about 8. The precipitate that was obtained was washed thoroughly with distilled water until chloride ion was not detected, and was dried at room temperature for 12 h. The dried precipitate was ground to a powder smaller than 100 mesh.

Samples containing various content of chromium were prepared by dry impregnation of powdered $Zr(OH)_4$ with aqueous solution of $(NH_4)_2CrO_4$ followed by calcining at high temperature for 1.5 h in air. These series of catalysts are denoted by their weight percentage of chromium and calcination temperature. For example, 1-CrO_x/ZrO_2-600 indicates the catalyst containing 1 wt.% chromium calcined at 600°C.

2.2. Procedure

Catalytic activities for *n*-hexane reactions over CrO_x/ZrO_2 were measured in a pulse microreactor constructed of 1/4 inch stainless-steel. For each experiment, 0.08 g of catalyst was loaded into a reactor. The reactor was packed with quartz chips that both positioned the catalyst sample near an external thermocouple and served as a preheating stage for the reactant gas. The catalyst samples were activated in situ by heating them under flowing He gas for 2 h at various temperature. Pulses of 1 μl reactant were injected into a He gas stream which passed over 0.08 g catalyst at 20 ml/min. The *n*-hexane reactions were carried out at 300–700°C. Reaction products were analyzed by gas chromatography equipped with a Bentone 34 on chromosorb W column at 130°C. Catalytic activity was represented as μmol of reacted *n*-hexane per g catalyst. Conversions for *n*-hexane reactions were taken as the average of the fourth to tenth pulse value.

The acid strength of the catalysts was measured qualitatively after pretreatments using a series of Hammett indicators [19–21]. The catalysts were pretreated in glass tubes by the same procedure as for the reactions. They were cooled to room temperature and filled with dry nitrogen. Color-changes in a series of indicators were observed for each catalyst by the spot test under dry nitrogen. Chemisorption of ammonia was employed to measure the acidity of catalysts. The amount of chemisorption was obtained as an irreversible adsorption of ammonia [23,24]. The specific surface area was determined by applying the BET method to the adsorption nitrogen at −196°C.

3. Results and discussion

3.1. Surface area

The specific surface areas of samples calcined at 600°C for 1.5 h are plotted as a function of chromium content in Fig. 1. The presence of chromium oxide strongly influences the surface area in comparison with the pure ZrO_2. Specific surface areas of CrO_x/ZrO_2 samples are much larger than that of pure ZrO_2 calcined at the same temperature, showing that surface area increases gradually with increasing chromium content. It seems likely that the interaction between chromium oxide and ZrO_2 protects catalysts from sintering. The dependence of the antisintering effect on chromium oxide content is clear from Fig. 1. These results are correlated with the fact that the transition temperature of ZrO_2 from amorphous to tetragonal phase increases with increasing chromium oxide content in DTA and XRD experiments reported previously [22,25].

3.2. Acidic properties of catalysts

The acid strength of the catalysts was examined by a color change method, using Hammett indicator in sulfuryl chloride [19–21,26]. Since it was very difficult to observe the color of indicators adsorbed on catalysts of high chromium oxide content, a low percentage of chromium content (0.1 wt.%) was used in this experiment. However, in the case of catalyst having high content of chromium (5 wt.%), a sample diluted with inert material, SiO_2, was used. Regardless of chromium content, the same results were obtained, as listed in Table 1. In this table, (+) indicates that the color of the base form was changed to that of the conjugated acid form. ZrO_2 evacuated at 400°C for 1 h has an acid strength of $Ho \leq +1.5$, while CrO_x/ZrO_2 was estimated to have a $Ho \leq -14.5$, indicating the formation of new acid sites stronger than those of single oxide components. The acid strength of CrO_x/ZrO_2 oxidized with O_2 at 500°C was also found to be $Ho \leq -14.5$, while CrO_x/ZrO_2 reduced with CO at 500°C was estimated to have a $Ho \leq -8.2$. Acids stronger than $Ho \leq -11.93$, which corresponds to the acid strength of 100% H_2SO_4, are superacid [27]. Consequently, CrO_x/ZrO_2 catalysts, except for reduced sample, would be solid superacids. The superacidic property is attributed to the double bond nature of the Cr=O in the complex formed by the interaction of ZrO_2 with chromate as:

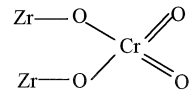

in analogy with the case of ZrO_2 modified with sulfate ion [19–21].

The acidity of catalysts, as determined by the amount of NH_3 irreversibly adsorbed at 230°C [22], is plotted as a function of the chromium content in Fig. 2. Although pure ZrO_2 shows the acidity of 0.05 meq/g, 1-CrO_x/ZrO_2 resulted in a remarkable increase in acidity (0.1 meq/g). As shown in Fig. 2, the acidity increases abruptly upon the addition of 1 wt.% chromium to ZrO_2, and then the acidity increases very gently with increasing chromium oxide content. Many combinations of two ox-

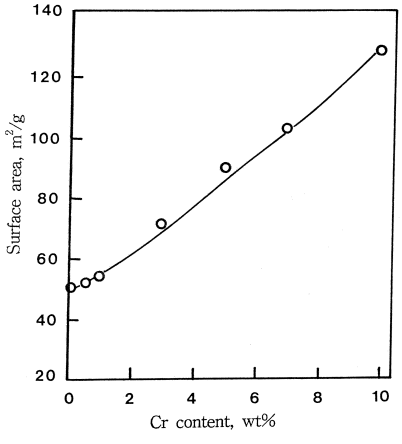

Fig. 1. Variation of surface area of CrO_x/ZrO_2 calcined at 600°C with chromium content.

Table 1
Acid strength of CrO_x/ZrO_2 and ZrO_2

Hammett indicator	pK_a value of indicator	CrO_x/ZrO_2[a]	CrO_x/ZrO_2[b]	CrO_x/ZrO_2[c]	ZrO_2
Benzenazodiphenyl-amine	+1.5	+	+	+	+
Dicinnamalacetone	−3.0	+	+	+	−
Benzalacetophenone	−5.6	+	+	+	−
Anthraquinone	−8.2	+	+	+	−
Nitrobenzene	−12.4	+	+	−	−
2,4-Dinitrofluorobenzene	−14.5	+	+	−	−

[a]Calcined in air at 600°C.
[b]Oxidized with O_2 at 500°C.
[c]Reduced with CO at 500°C.

ides have been reported to generate acid sites on the surface [28–30]. The combination of ZrO_2 and CrO_x probably generates stronger acid sites and more acidity as compared with the separate components. A mechanism for the generation of acid sites by mixing two oxides has been proposed by Itoh et al. [28]. They suggest that the acidity generation is caused by an excess of a negative or positive charge in a model structure of a binary oxide related to the coordination number of a positive element and a negative element.

Infrared spectroscopic studies of pyridine adsorbed on solid surfaces have made it possible to distinguish between Brönsted and Lewis acid sites [31], Fig. 3 shows the IR spectra of pyridine adsorbed on 1-CrO_x/ZrO_x evacuated at 500°C for 1 h. There were peaks at 1443, 1483, 1497, 1554, 1580, 1595 and 1605 cm^{-1} comprising the vibrational modes of pyridine after evacuation at room temperature. Many peaks were weakened after evacuation at 250°C. Consequently, this set of disappeared absorption peaks can be assigned to hydrogen-bonded pyridine [32]. This bands at 1554 and 1497 cm^{-1} are the characteristic peaks of pyridinium ion, which are formed on Brönsted acid sites [33]. The other set of absorption peaks at 1443, 1483, 1580 and 1605 cm^{-1} is contributed by pyridine coordinatively bonded to Lewis acid sites. It is clear that both Brönsted and Lewis acid sites exist on the surface of CrO_x/ZrO_2 catalysts calcined at 600°C.

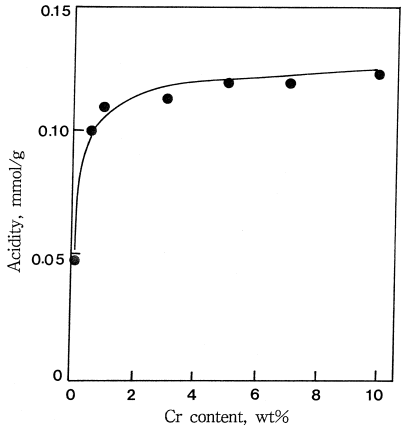

Fig. 2. Acidity of CrO_x/ZrO_2 against chromium content.

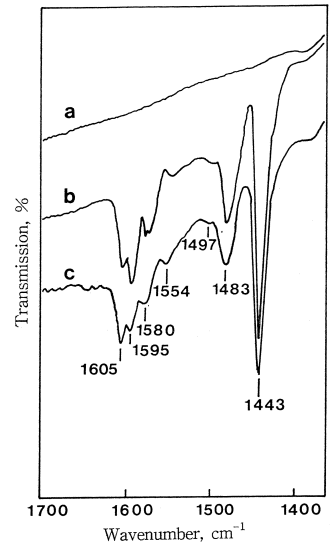

Fig. 3. IR Spectra of pyridine adsorbed on 1-CrO_x/ZrO_2: (a) background of 1-CrO_x/ZrO_2 after evacuation at 500°C for 1 h: (b) pyridine adsorbed on (a) sample followed by evacuating at 250°C for 1 h.

3.3. Catalytic behavior of CrO_x/ZrO_2

Chromium oxide catalysts exhibit different catalytic behavior depending on the oxidation state of chromium species supported on metal oxides [1–5]. We tested *n*-hexane reaction over chromium oxide–zirconia catalyst using a pulse technique so that the occurrence of two main catalytic reactions, cracking and dehydrocylization reactions was observed. Fig. 4 shows the variations of amount of products and reactant after *n*-hexane reaction over 3-CrO_x/ZrO_2-600 with pulse number. The products were identified to be benzene due to the dehydrocylization reaction and identified to be C_1 and C_2 hydrocarbons formed through the cracking reaction. As shown in Fig. 4, however, at the first pulse cracking reaction occurred more predominantly than dehydrocyclization reaction, while from the second pulse, dehydrocyclization reaction was enhanced remarkably, and then from the fourth pulse, catalytic activity for the reaction was nearly constant.

It has been known that cracking reaction for *n*-hexane takes place in strong acid sites of the catalysts [34,35], while the active site for the dehydrocyclization reaction of *n*-hexane is Cr^{3+} [36]. The predominant cracking reaction of *n*-hexane at the first pulse can be explained from the fact that chromium oxide catalyst calcined at 600°C has strong acid site because chromium species bonded to zirconia surface is mainly present as chromate (Cr^{6+}). As described above, CrO_x/ZrO_2 calcined at 600°C has an acid strength of $Ho \leq -14.5$ and the main presence of chromate (Cr^{6+}) for the calcined sample was demonstrated in XPS and IR results reported previously [22].

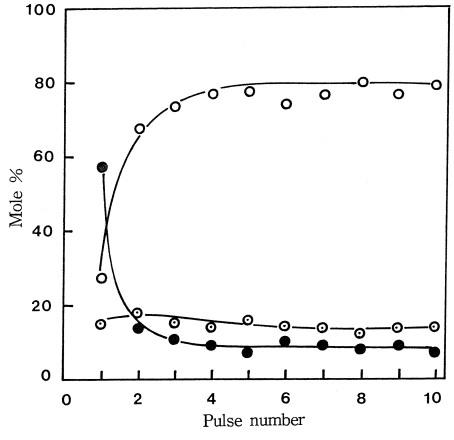

Fig. 4. Variation of mol% of products and reactant after *n*-hexane reaction over 3-CrO_x/ZrO_2-600 with pulse number. ○: Benzene, ●: cracking product, ⊙: *n*-hexane.

The remarkable enhancement of dehydrocyclization reaction and concomitant decrease of cracking reaction for *n*-hexane from the second pulse is responsible for the reduction of chromium species from +6 to +3 during *n*-hexane reaction. Namely, it seems likely that hydrogen produced through dehydrocyclization reaction of *n*-hexane makes reduction of chromium species from +6 to +3. It was reported that supported chromium oxide is easily reduced by olefins or alcohol [37,38]. To obtain further information on oxidation state, the XPS in the Cr $2P_{3/2}$ region was analyzed [22]. Ten pulses of 1 μl of *n*-hexane were injected successively into a He gas stream which passed over 0.08 g of sample calcined at 600°C at 15 ml/min, where reaction temperature was 600°C. The concentration of Cr^{3+} species for the sample calcined at 600°C was 46%, while that of Cr^{3+} species after reaction with *n*-hexane was found to be 89%. From the above results, it is clear that active site for dehydrocyclization reaction of *n*-hexane is Cr^{3+} [36]. As listed in Table 1, CrO_x/ZrO_2 reduced with CO has an acid strength of $Ho \leq -8.2$, indicating that the oxidation state of chromium species influences the acid strength and subsequent catalytic activities.

As shown in Fig. 4, CrO_x/ZrO_2 catalyst is active for the dehydrocyclization reaction of *n*-hexane. Fig. 5 shows the catalytic activity of 1-CrO_x/ZrO_2-600 for the dehydrocyclization reaction as a function of reaction temperature. The catalyst began to exhibit catalytic activity at 350°C, giving a maximum at 600°C. The samples calcined at other temperatures exhibited

catalytic behavior similar to that calcined at 600°C, also giving a maximum at 600°C.

Catalytic activities of CrO_x/ZrO_2-600 and CrO_x/ZrO_2-700 for dehydrocyclization reaction are plotted as a function of chromium content in Fig. 6. Although pure ZrO_2 showed no catalytic activity, the addition of 1 wt.% chromium to ZrO_2 resulted in a remarkable increase in activity, indicating that chromium element for dehydrocyclization reaction is indispensable. As shown in Fig. 6, the activities increase abruptly upon the addition of chromium to ZrO_2 and then the activities increase very gently with increasing chromium oxide content. The patterns of catalytic activities in Fig. 6 are very similar to that of acidity in Fig. 2 except for pure ZrO_2. These results suggest that catalytic activity for dehydrocyclization and acidity of CrO_x/ZrO_2 are correlated with the content of chromium oxide.

The use of chromia–alumina as a catalyst for the dehydrogenation and dehydrocyclization of hydrocarbons has been studied extensively [36,39]. Therefore, on the basis of extensive research carried out on a variety of hydrocarbons, the mechanism of dehydrocyclization of alkanes is now well-understood. In the case of chromium oxide–zirconia, it seems likely that chromium oxide acts as a catalyst for the dehydrogenation and for the double bond isomerization, similar to the mechanism proposed previously [40].

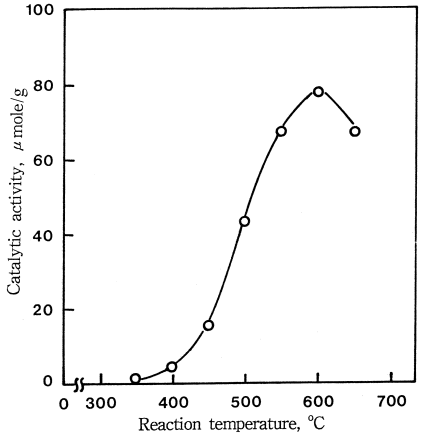

Fig. 5. Catalytic activity of 1-CrO_x/ZrO_2-600 for *n*-hexane dehydrocyclization reaction as a function of reaction temperature.

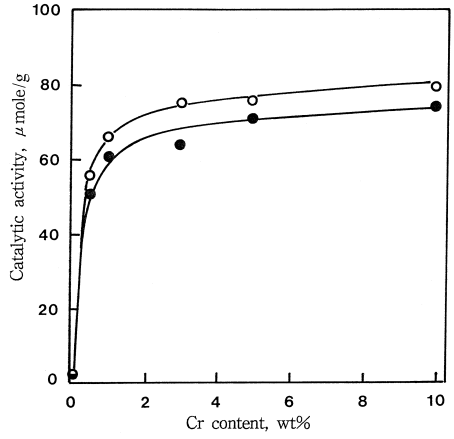

Fig. 6. Catalytic activity for *n*-hexane dehydrocyclization reaction as a function of chromium content. ○: CrO_x/ZrO_2-600, ●: CrO_x/ZrO_2-700.

3.4. Cyclic behavior of catalytic activity

From the results of XPS [22] and the analysis of products in Fig. 4, it is clear that Cr^{6+} species on the catalyst surface during *n*-hexane reaction is easily reduced to Cr^{3+} species. Also, previously, it was reported that Cr^{3+} species reduced with CO or H_2 was easily reoxidized to Cr^{6+} species by treatment with O_2, which was demonstrated by XPS and IR [22]. Therefore, it is expected that catalyst reduced with reactant, *n*-hexane can be reoxidized by treating reduced sample with O_2. To examine cyclic behavior of catalytic activity depending on redox state of chromium species, a pulse micro-reactor was used and results are illustrated in Figs. 7 and 8.

Fig. 7 shows cyclic behavior of catalytic activity for *n*-hexane cracking reaction at 550°C. As shown in Fig. 7, at the first pulse, cracking activity is very high, but from the second pulse, cracking activity drops suddenly because Cr^{6+} species is reduced to Cr^{3+} species during *n*-hexane reaction. Black circle in Fig. 7 indicates the cracking activity of CrO_x/ZrO_2 after reduction with 20 ml H_2 at 550°C, showing very low

cracking activity. However, after the 7th pulse, we treated the sample with 20 ml of O_2 and then at the 8th pulse, cracking activity was measured. Arrow (↑) in Fig. 7 indicates the interval of 20 ml O_2 injection. At the 8th pulse, cracking activity was completely recovered, but at the 9th pulse, cracking activity dropped suddenly due to the reduction of Cr^{6+} species as done at the second pulse. As shown in Fig. 7, catalytic behavior as this was repeated at every pulse after 20 ml O_2 injection, indicating that redox cycles of chromium species are reversible. In view of XPS results, acid strength measurement, and above cyclic behavior of cracking activity, it is concluded that the catalyst having Cr^{6+} species are responsible for the cracking reaction of *n*-hexane.

Fig. 8 shows cyclic behavior of catalytic activity for the dehydrocyclization reaction of *n*-hexane. As shown in Fig. 8, at the first pulse, dehydrocyclization activity is very low, but from the second pulse, activity increases steeply because Cr^{3+} species from Cr^{6+} species was formed by the reduction of H_2 produced during *n*-hexane reaction. Black circle in Fig. 8 shows the dehydrocyclization activity of CrO_x/ZrO_2 after reduction with 20 ml H_2 at 550°C, giving very high activity. However, after the 7th pulse, we oxidized the catalyst with 20 ml of O_2, as done in Fig. 7, and then at the 8th pulse dehydrocyclization activity was estimated. Arrow (↑) in Fig. 8 indicates the interval of 20 ml O_2 injection. At the 8th pulse, dehydrocyclization activity dropped suddenly, but at the 9th pulse, activity was nearly recovered due to the reduction of Cr^{6+} species, as done at the second pulse. As shown in Fig. 8, catalytic behavior as this was repeated at every pulse after 20 ml O_2 injection, indicating the reversible and cyclic redox behavior of CrO_x/ZrO_2. From these results and XPS results, it seems likely that active site for the dehydrocyclization reaction of *n*-hexane is Cr^{3+} species.

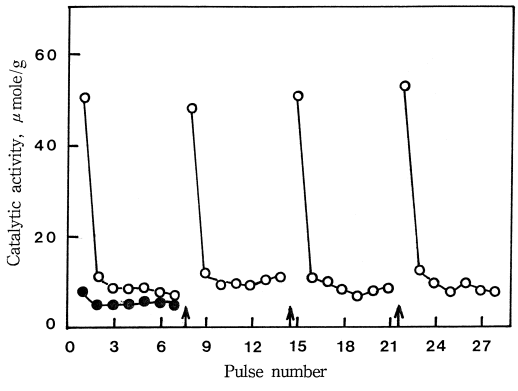

Fig. 7. Cyclic behavior of catalytic property of 1-CrO_x/ZrO_2-600 for *n*-hexane cracking reaction, where arrow (↑) indicates the interval of 20-ml O_2 injection and black circle (●) indicates catalytic activity after reduction with 20 ml H_2 at 550°C.

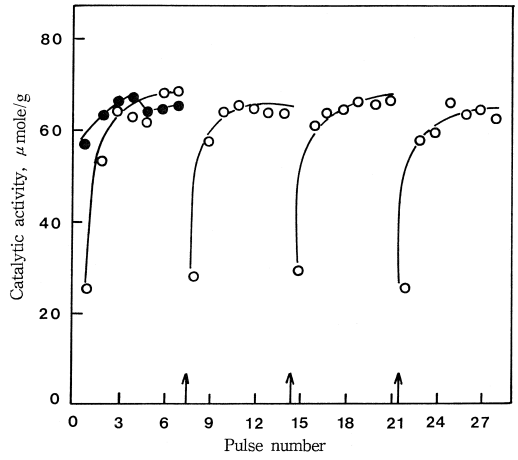

Fig. 8. Cyclic behavior of catalytic property of 1-CrO_x/ZrO_2-600 for *n*-hexane dehydrocyclization reaction, where arrow (↑) indicates the interval of 20-ml O_2 injection and black circle (●) indicates catalytic activity after reduction with 20 ml H_2 at 550°C.

4. Conclusions

The presence of chromium oxide strongly influences the surface area in comparison with the pure ZrO_2 because the interaction between chromium oxide and ZrO_2 protects catalyst from sintering. As a consequence, the surface area of CrO_x/ZrO_2 increased gradually with increasing chromium oxide content. Upon the addition of only a small amount of chromium oxide to ZrO_2, both the activity and acid strength of catalyst increased remarkably, showing the

presence of Brönsted and Lewis acid sites on the surface of CrO_x/ZrO_2.

The catalytic behavior of CrO_x/ZrO_2 was investigated by reacting *n*-hexane as a test reactant using a pulse technique. Cr^{6+} species existing on the surface of catalyst was responsible for the formation of strong acid site and cracking activity of *n*-hexane, while Cr^{3+} species was responsible for the dehydrocyclization activity of *n*-hexane. However, the Cr^{6+} species was easily reduced to Cr^{3+} species during the catalytic reaction of *n*-hexane and the reduced Cr^{3+} species was also easily reoxidized by treating with O_2. Cyclic catalytic and redox behavior of CrO_x/ZrO_2 were reversible.

Acknowledgements

This work was supported by the Korea Science and Engineering Foundation through the Research Center for Catalytic Technology at Pohang University of Science and Technology.

References

[1] J.P. Hogan, J. Polym. Sci. 8 (1970) 2637.
[2] D.L. Myers, J.H. Lunsford, J. Catal. 99 (1986) 140.
[3] A. Clark, Catal. Rev. 3 (1969) 145.
[4] C. Groeneveld, P.P.M.M. Wittgen, A.M. van Kersbergen, P.L.M. Mestrom, C.E. Nuijten, C.E. Schuit, J. Catal. 59 (1979) 153.
[5] M. Shelef, K. Otto, H. Gandhi, J. Catal. 12 (1968) 361.
[6] M.P. McDaniel, Adv. Catal. 33 (1985) 47.
[7] G. Ghiotti, E. Garrone, A. Zecchina, J. Mol. Catal. 46 (1988) 61.
[8] W. Hill, G. Öhlmann, J. Catal. 123 (1990) 147.
[9] A. Cimino, D. Cordischi, S. De Rossi, G. Ferraris, D. Gazzoli, V. Indovina, G. Minelli, M. Occhiuzzi, M. Valigi, J. Catal. 127 (1991) 744, 761, 777.
[10] T. Yamaguchi, M. Tan-no, K. Tanabe, Preparation of Catalysts V, Elsevier, 567 (1991).
[11] M. Hino, K. Arata, J. Chem. Soc. Chem. Commun. 1355 (1987) .
[12] M.Y. He, J.G. Ekerdt, J. Catal. 90 (1984) 17.
[13] T. Maehashi, K. Maruya, K. Domen, K. Aika, T. Onishi, Chem. Lett. 747 (1984) .
[14] T. Yamaguchi, H. Sasaki, K. Tanabe, Chem. Lett. 1017 (1973) .
[15] B.H. Davis, P. Ganesan, Ind. Eng. Chem. Prod. Res. Dev. 19 (1979) 191.
[16] T. Iizuka, Y. Tanaka, K. Tanabe, J. Catal. 76 (1982) 1.
[17] P. Turlier, J.A. Dalmon, G.A. Martin, Stud. Surf. Sci. Catal. 11 (1982) 203.
[18] R. Szymanski, H. Charcosset, P. Gallezot, J. Massardier, L. Tournayan, J. Catal. 97 (1986) 366.
[19] J.R. Sohn, H.J. Kim, J. Catal. 101 (1986) 428.
[20] J.R. Sohn, H.W. Kim, J.T. Kim, J. Mol. Catal. 41 (1987) 379.
[21] J.R. Sohn, H.W. Kim, J. Mol. Catal. 52 (1989) 361.
[22] J.R. Sohn, S.G. Ryu, Langmuir 9 (1993) 126.
[23] J.R. Sohn, A. Ozaki, J. Catal. 61 (1980) 29.
[24] J.R. Sohn, H.J. Jang, J. Mol. Catal. 64 (1991) 349.
[25] J.R. Sohn, S.G. Ryu, M.Y. Park, Y.Il. Pae, J. Mater. Sci. 28 (1993) 4651.
[26] L.P. Hammett, A.J. Deyrup, J. Am. Chem. Soc. 54 (1932) 2721.
[27] F.G.A. Olah, G.K.S. Prakash, J. Sommer, Science 206 (1979) 13.
[28] M. Itoh, H. Hattori, K. Tanabe, J. Catal. 35 (1974) 225.
[29] V.A. Dzisko, Proc. 3rd Int. Congr. Catalysis, Vol. 1, No. 19, Amsterdam (1964).
[30] M. Miura, Y. Kubota, T. Iwaki, K. Takimoto, Y. Muraoka, Bull. Chem. Soc. Jpn. 42 (1969) 1476.
[31] E.P. Parry, J. Catal. 2 (1963) 371.
[32] M.C. Kung, H.H. Kung, Catal. Rev. Sci. Eng. 2 (1985) 425.
[33] G. Connell, J.A. Dumesic, J. Catal. 105 (1987) 285.
[34] S.J. Decanio, J.R. Sohn, P.O. Fritz, J.H. Lunsford, J. Catal. 101 (1986) 132.
[35] J.R. Sohn, S.J. Decanio, P.O. Fritz, J.H. Lunsford, J. Phys. Chem. 90 (1986) 4847.
[36] W. Grünert, W. Saffert, R. Feldhaus, K. Anders, J. Catal. 99 (1986) 149.
[37] W. Hill, G. Ohlmann, J. Catal. 123 (1990) 147.
[38] M.B. Leonard, W.L. Carrick, J. Org. Chem. 33 (1968) 616.
[39] H. Pines, C.T. Goetschel, J. Org. Chem. 30 (1965) 3530.
[40] H. Pines, The Chemistry of Catalytic Hydrocarbon Conversion, Academic Press, New York, 1981, pp. 185–212.